Electric Power Systems Research 171 (2019) 127–140

Contents lists available at ScienceDirect

Electric Power Systems Research

journal homepage: www.elsevier.com/locate/epsr

Exploiting network topology optimization and demand side management to improve bulk power system resilience under windstorms

Yanlin Li[a], Kaigui Xie[a], Lingfeng Wang[b], Yingmeng Xiang[c]

[a] State Key Laboratory of Power Transmission Equipment and System Security, Chongqing University, Chongqing 400044, China
[b] Department of Electrical Engineering and Computer Science, University of Wisconsin-Milwaukee, Milwaukee, WI 53211, USA
[c] GEIRI North America, San Jose, CA, 95134, USA

ARTICLE INFO

Keywords:
Power system resilience
Demand response
Weather condition based real time pricing
Network topology optimization
Extreme weather conditions

ABSTRACT

Natural hazards are great threats to the safe and reliable operation of electric power systems. Some high-impact low-probability (HILP) events usually cause severe load losses to the power grid. Therefore, the enhancement of power system resilience appears to be particularly important. Nowadays, novel smart grid technologies provide more flexible ways for the power system operation. However, these technologies are not comprehensively incorporated in the resilience assessment framework to quantify their contribution for resilience enhancement. In this paper, fragility models for transmission lines and towers and sequential wind data are applied to simulate the operational states of power system under windstorm events. Then, a demand side management (DSM) program termed weather condition based real time pricing (WCRTP) framework is proposed to regulate the customer's electricity consumption behavior according to the extreme weather conditions. A network topology optimization (NTO) operation strategy is applied to mitigate the transmission congestion and realize the potential of transmission capacity by optimizing the network topology. The sequential Monte Carlo Simulation (MCS) method based resilience enhancement evaluation framework is developed to incorporate WCRTP and NTO. Numerical case studies are performed on modified RTS-79 systems. Both methods are proved to be effective self-adaptive measures for power systems in both customer behavior regulation aspect and transmission strategy aspect to boost the system resilience, which could eventually help power system operators to deal with the natural hazards in a more flexible, resourceful, and reliable manner.

1. Introduction

As one of the most critical infrastructures in the world, power system's resilience in the face of extreme weather conditions is attracting more and more attention due to its critical role in maintaining social stability and economic development. As these unforeseeable high-impact low-probability (HILP) events cannot be easily integrated into the power system planning process, they could cause great economic losses to all sectors of the society [1,2]. Therefore, the study of resilience enhancement measures of power systems is of great importance and will contribute to the safe and reliable operation of power systems in the presence of adverse, extreme events.

Resilience is the capability of electric power system to withstand high impact, low probability disturbances, such as natural hazards and attacks, speedily recover from the disruptive events, adapt its operational modes to continue the energy delivery service and prevent or relieve the negative impact from the shock [3–5]. According to the report of National Infrastructure Advisory Council (NIAC) in the U.S., the resilience features contain robustness, resourcefulness, rapid recovery, and adaptability [3]. The concept and study of power system resilience under natural hazards are reviewed in Refs. [5,6]. In Ref. [7], the consensus of the definition and taxonomy for power system resilience is summarized in detail. The resilience enhancement measures under extreme events are an emerging topic in the recent years. In Refs. [8] and [9], the resilience characteristics are incorporated into the power system planning process, which aims to enable the transmission grid and distribution system to withstand the natural hazards in a more robust manner. The general timeline of response for utilities to bolster the electric grid resiliency under natural hazards includes hardening and resilience investment, emergency response and corrective actions, damage assessment and restoration [6]. Prior to the presence of extreme weather, the hardening measure is an effective way to boost the resiliency by upgrading the system to have a more robust structure, which is studied in Refs. [10] and [11]. After receiving alerts for the forecasted disruptive events, some proactive operation strategies can be adopted to reduce the system risk, such as generation re-dispatch

E-mail addresses: yanlinli1991@gmail.com (Y. Li), kaiguixie@vip.163.com (K. Xie), l.f.wang@ieee.org (L. Wang), yingmeng.xiang@geirina.net (Y. Xiang).

https://doi.org/10.1016/j.epsr.2019.02.014
Received 4 September 2018; Received in revised form 27 January 2019; Accepted 12 February 2019
Available online 23 February 2019
0378-7796/

[12,13] and resilience-oriented proactive micro-grid management [14,15]. Other resilience enhancement measures such as distribution automation technologies [16], defensive islanding [17], mobile emergency generator [18], optimal switch placement in distribution systems [19] and transportable energy storage systems [20] can be deployed in the power grid to make it more resilient to the extreme weather. In the post-disaster state, the quick and efficient restoration process is also a key requirement for a resilient system which can help reduce the losses. A post-disaster decision making model is established in Ref. [21] to obtain the optimal repair arrangement, unit commitment solution, and configuration for the system during the restoration period of power grid. A resilience-oriented service restoration method using micro-grids and a distribution system restoration decision support tool are developed in Refs. [22] and [23], respectively. In Ref. [24], a hierarchical response-based approach based on the synchrophasor technology is proposed to facilitate the restoration procedure of electric power systems. With increasing interactions between multiple energy sectors, multi-energy system has attracted more attention of the researchers in energy research field. The study of multi-energy system and its resilience enhancement issues are presented in Refs. [25–27].

There has also been some literature which focuses on the resilience evaluation framework and resilience metrics [7,28–32]. Power system resilience can be quantified to be the ratio of the area between the real and expected performance curves [7,28,29]. In Ref. [7], the resilience triangle for the system performance is applied to calculate the system resilience metrics. In Ref. [28], a quantitative framework for evaluating the resilience of micro-grid is proposed. In this framework, windstorm profiles and fragility curves of overhead distribution branches are utilized to quantify the degradation in the micro-grid performance. Degradation index (DI), restoration efficiency index (REI) and micro-grid resilience index (MRI) are established to describe the system resilience performance during an extreme event. In Ref. [30], a Monte Carlo simulation (MCS) and fragility model based quantification framework for resilience is presented. Specific reliability indices including Loss of Load Frequency (LOLF), Expected Energy Not Supplied (EENS) and infrastructure indices are utilized to quantify the system resilience towards extreme weather situations. In Ref. [31], the reliability indices including Loss of Load Probability (LOLP) and Expected Demand Not Supplied (EDNS) are also applied to evaluate the power system resilience enhancement performance when micro-grids are integrated into power systems in the face of extreme events. In Ref. [32], the concepts of operational resilience and infrastructure resilience are introduced and the corresponding metrics are established to quantify the system resilience during different phases of extreme weather events.

The new smart grid technologies boost the flexibility of power system operation, which could enable the power system to be more resilient to extreme weather conditions [6]. DSM could be regarded as an effective way to utilize the flexibility from customer response aspect to enhance the system resilience against extreme weathers [6,33]. At the same time, some network topology optimization technologies, such as reconfiguration of network topology [6] and dynamic circuit reconfiguration [34], are also regarded as potential resiliency improvement measures to realize the flexibility of transmission infrastructure. This paper is focused on the study of these novel smart grid technologies and the quantification of their resilience enhancement contributions in the presence of natural hazards.

Demand side management (DSM) is an effective measure to regulate the energy consumption behavior of customers by price elasticity mechanism and well-organized operation strategies. The basic concepts and detailed literature review about DSM is introduced in Refs. [35,36]. DSM has been implemented into many aspects of power system including optimal operation, frequency control, system security, renewable integration, risk management and planning, etc. [37–42]. The objectives of DSM implementation include postponement of generation and transmission asset upgrades, security and stability improvement, reliability enhancement, efficient utilization of the power market and reduction of electricity price for customers etc. [43]. It is verified that the deploy of DSM will contribute to the system congestion management [44] and generation capacity adequacy [45], which is meaningful for the reliable operation of power system especially in those unforeseen extreme weather event. In Ref. [46], experiences and lessons learned from Japan is presented and demand response is considered as a countermeasure against power loss and is utilized to improve electricity supply continuity. However, limited work has been conducted to study and quantify the resilience enhancement performance of DSM under extreme weather conditions. At the same time, it would perform better if the pricing mechanism of DSM programs is adjusted to trace the extreme weather conditions itself or the severity of its consequence to meet the adaptability requirements for the resilient system.

As for the transmission topology aspect, under state-of-the-art transmission technology condition, the transmission topology can be optimized based on operational characteristic of power system and the transmission assets will be dispatchable to relieve transmission congestions, which can further lead to the reduction of operational cost and relieve load curtailment when there is component failure or emergency in the system. One practical and commonest way to change the transmission topology can be implemented by switching on/off the transmission lines. The idea of dispatchable lines called optimal transmission line switching is put forward in Ref. [47] and is mathematically illustrated as a mixed integer linear programming problem in Ref. [48]. Many work has been conducted to fulfill multiple operating purpose by means of OTS. In Ref. [49], the OTS is incorporated in dispatch to cut the cost while satisfying N-1 criterion. Probabilistic security analysis of OTS is studied in Ref. [50]. In Ref. [51], a rotor stress controlled OTS is applied as an effective method to relieve congestion. A co-optimization formulation of unit commitment and OTS is presented in Ref. [52]. The OTS incorporated power system expansion planning is proposed in Refs. [53] and [54], which conclude that OTS will affect the optimal expansion plan and increase wind power penetration. In Ref. [55], OTS is proven to be an effective way to mitigate the adverse impact of geomagnetically induced currents to the power system operation. Another powerful tool to change network topology and mitigate network congestion is busbar reconfiguration in high voltage substations [56]. In practice, the generators, transmission lines and loads are all connected with busbars by switchable devices like circuit breakers, the dispatchable states of switching equipment, such as busbar switching, can realize the reconfiguration of transmission network. In Refs. [57] and [58], the busbar switching is implemented in the power system operation as an effective overload relieving measure. In Ref. [59], a comprehensive network reconfiguration technology which contains both OTS and optimal busbar switching is established named network topology control (NTO). It should be noted that the implementation of NTO doesn't require great additional investment in the upgrade of existing transmission assets. When natural hazard happens, the outage of power system components will make the power system suffer from a severe congestion level. The operation economy and reliability levels will decrease significantly. The enforcement of NTO operation strategies will realize the potential transmission capacity, relieve congestion levels and reduce the load curtailment, which make the system more resilient to the natural hazards. There is limited study on utilizing the flexibility of transmission network which survive under the extreme weather conditions to boost the system resilience on the bulk power system level. In Ref. [12], the coordination of generator re-dispatch and line switching is utilized as emergency response to enhance power grid resilience. However, the bus splitting which is a promising network reconfiguration mechanism is not considered to study the contribution of network topology optimization to the resilience enhancement performance comprehensively.

As both DSM and NTO have inner logical connection in utilizing flexible operation strategy to alleviate congestions of power system under smart grid circumstance, which will contribute to the resilience enhancement of power system when extreme weather condition

happens, this paper aims to quantify their resilience improvement performance and provide potential operation scheme for the system. The main contributions of this paper are:

1) Smart grid technologies are applied as resilience enhancement measures of power system which can realize the self-adaptive ability of power system under extreme weather conditions from both customer aspect and transmission topology aspect.
2) The concept of weather condition-based demand response program pricing mechanism is studied to regulate the energy consumption behavior of customers during windstorm.
3) The comprehensive network topology optimization technology including both transmission switching and substation bus splitting mechanism is first applied to realize the potential of transmission network survived in the natural hazard to boost the system resilience by the optimization of flexible transmission topology.
4) The MCS method and proposed evaluation methodology can capture the correlation between load response characteristic from DSM, the operational benefit of NTO, power system operational characteristic and sequential weather conditions systematically, which will lead to an accurate resilience enhancement assessment result.

The rest of the paper is organized as follows: fragility model of transmission infrastructures and system state simulations are discussed in Section 2; the demand side management modeling and weather condition based pricing mechanism are presented in Section 3; the NTO technology is introduced in Section 4; the resilience enhancement evaluation procedure is discussed in Section 5; case studies are presented in Section 6; conclusion and future work are introduced in Section 7.

2. Fragility model of transmission infrastructures and system state simulation

To study the power system resilience under natural hazards, the stochastic behavior of weather conditions with respect to the sequential and regional characteristic should be captured and their impact on the power system should be simulated. Therefore, fragility model of components and the state simulation of transmission elements in the power system are introduced as follows.

2.1. Fragility curves of transmission lines and towers

The main research object of natural hazard of this paper is windstorms. As failure rate of transmission infrastructures are relevant to the wind speed, therefore, a fragility model of transmission lines and transmission towers which is shown in Fig.1 Ref. [30] is used to simulate the states of transmission components under multi-temporal and multi-regional windstorm conditions.

Due to the stochastic characteristic of wind and its complex influence mechanisms towards the power system components, the resilience enhancement evaluation is a complicated issue involving many aspects like collection of meteorological data, system state simulation, engineering structure analysis of transmission infrastructures, power system operation etc. Furthermore, the main purpose of this paper is to quantify the resilience enhancement performance of smart grid technologies instead of improving existing power system model under natural hazard circumstance. Therefore, some appropriate approximations [30] are adopted to reduce the complexity of the problem while considering the main operational characteristic of the system and maintaining the feasibility and effectiveness of resilience enhancement assessment, which are illustrated in the following.

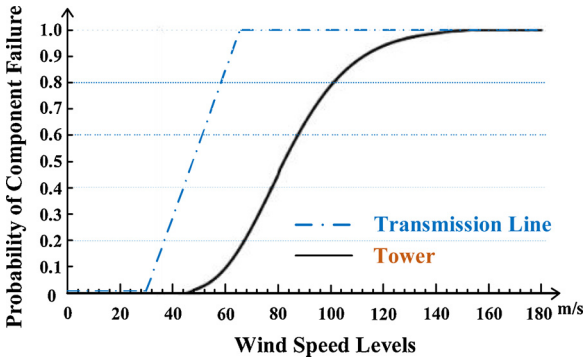

Fig. 1. Fragility curves of transmission lines and towers.

All towers and transmission lines are supposed to share the same fragility curves. The operation of generating unit is supposed not to be influenced by the windstorm, but it can still be disconnected because of the transmission corridor failures. As this paper aims to study the contribution of DSM in the resilience enhancement aspect at the macro level, therefore, initial load demand is assumed to be weather-independent. When a transmission corridor is being repaired, new outage on this corridor is not considered. Since it is difficult to simulate the weather condition for each transmission corridor with accurate spatial and temporal data, the test system is divided into multiple regions. Within each region, it is considered to share the same weather condition. The transmission corridor is considered to go through different weather regions where its from-side bus and to-side bus are located. Furthermore, as there is lack of enough restoration time information in engineering practice for the transmission corridors being collapsed or damaged under natural hazards [62], the repair time is based on expert judgement.

2.2. Fragility modeling of transmission lines

There are multiple reasons for the transmission line failures relating to the weather conditions, such as windage yaw discharge, shackle failure, etc. The line fragility curve which describes the relationship between the failure probability of a line and corresponding wind speed is shown in Fig. 1, and it can be expressed as follows [30]:

$$F_{P,L}(v) = \begin{cases} \tilde{F}_{P,L\_nws} & v < v_{critical\_L} \\ F_{P,L\_hws}(v) & v_{critical\_L} \le v < v_{inevitable\_L} \\ 1 & v \ge v_{inevitable\_L} \end{cases} \quad (1)$$

where $F_{P,L}(v)$ is the failure probability of transmission line under wind speed v, $\tilde{F}_{P,L\_nws}$ refers to the failure probability under normal wind speed conditions, $F_{P,L\_hws}(v)$ represents that, at high speed levels, the failure probability of the line is considered as a function to the wind speed v, $v_{critical\_L}$ is the critical wind speed when the line's failure probability begins to pick up, $v_{inevitable\_L}$ is the speed at which the line has inevitable probability to be in the outage state. The utilized $v_{critical\_L}$ is in accordance with a statistic analysis illustrated in Ref. [60]. Between $v_{critical\_L}$ and $v_{inevitable\_L}$, which are considered as 30 m/s and 60 m/s respectively, the failure probability of transmission lines grows with the increase of the wind speed and they follow the linear relationship.

2.3. Fragility modeling of tower

The tower fragility modelling is established by the analysis of structural simulation model for the UK National Grid L2 transmission tower. The tower fragility curve under multiple wind loadings is formulated by the analysis of material and geometrical nonlinearities, which is shown in Fig. 1 and is illustrated as follows [30]:

$$F_{P,T}(v) = \begin{cases} 0 & v < v_{critical\_T} \\ F_{P,T\_hws}(v) & v_{critical\_T} \le v < v_{inevitable\_T} \\ 1 & v \ge v_{inevitable\_T} \end{cases} \quad (2)$$

where $F_{P,T}(v)$ is the failure probability of tower under wind speed v, $F_{P,T\_\_hws}(v)$ indicates the failure probability of tower at high wind speed levels, $v_{critical\_T}$ is the critical wind speed when the tower's failure probability begins to pick up, $v_{inevitable\_T}$ is the speed at which the tower has inevitable probability to collapse. When the transmission corridor is connected by towers in series, the outage of whole corridor can be caused by the collapse of any individual tower. Therefore, the failure probability $F_{P\_Corridor}$ of a transmission corridor is:

$$F_{P\_Corridor} = 1 - P(S_{T,1} = 1) \times P(S_{T,2} = 1) \times \ldots \times P(S_{T,N} = 1) \tag{3}$$

where $S_{T,a}$ is the state of a-th tower (0: collapse, 1: survive), N is the total number of towers along transmission corridor which is determined by the corridors' length and the distance between towers. Based on the assumptions that the towers fail independently and follow equispaced arrangement, (3) can be simplified as follows:

$$F_{P\_Corridor} = 1 - \prod_{a=1}^{N} (1 - F_{P,T,a}) \tag{4}$$

where $F_{P,T,a}$ is the failure probability of the a-th tower.

2.4. States simulation of lines and towers

To fully integrate the operational characteristic of power system under natural hazard into the sequential MCS procedures, the failure states and corresponding repair time of lines and towers should also be determined. Either line failure or tower collapse can lead to the corridor outage. A double circuit failure can also happen when two circuits are on the same tower which collapses under windstorm circumstance.

In each simulation step, the failure probability of transmission lines and towers can be obtained dynamically based on the real-time wind speed data and fragility curves. Then based on the MCS methodology, the failure probability is compared with a uniformly distributed and dynamic random number, and the occurrence of an individual circuit outage can be judged by the equation as follows [70]:

$$LS(v_t, L_i) = \begin{cases} 1 & F_{P,L}(v_t) < \tau \\ 0 & F_{P,L}(v_t) > \tau \end{cases} \tag{5}$$

where $LS(v_t, L_i)$ refers to the state of i-th line (1: normal state, 0: failure state) when the wind speed is v_t and τ indicates the dynamic random number ($\tau \sim U(0,1)$). At the same time, a tower collapse can also lead to the outage of a transmission corridor (both single-circuit and double-circuit outage could happen), which can be determined by:

$$TS(v_t, T_i) = \begin{cases} 1 & F_{P,T}(v_t) < \tau \\ 0 & F_{P,T}(v_t) > \tau \end{cases} \tag{6}$$

where $TS(v_t, T_i)$ is the state of the i-th tower when the wind speed is v_t.

After the occurrence of line and tower failure, the repair time (RT) should be generated [70]. As the severity of the extreme weather conditions will affect the difficulty in maintenance seriously. Therefore, three severity degrees are considered here to reflect the impact of weather conditions towards the repair time, which includes mild, medium, and intense. The severity degrees are determined by the maximum wind speed of the wind profile in a windstorm event. Then the severity coefficient (SC) is generated as a uniformly distributed random factor within a severity-related predetermined range. The SC s are used to multiply the normal repair time RT_0 to get the repair time for each severity degrees. The RT_0 for the transmission lines and towers are assumed to be 10 h and 50 h respectively under normal weather conditions [61,62]. After the discussion with the system operator in State Grid Corporation of China ($SGCC$), three severity degrees are determined including, $v_{max} \leq 30$ m/s, $30 < v_{max} \leq 50$ m/s, $50 < v_{max} \leq 60$ m/s, which are corresponding to mild, medium, and intense severity degrees. The repair time under three severity degrees could be calculated as follows [30]:

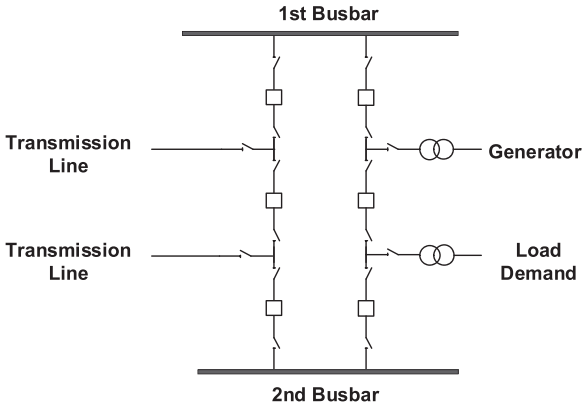

Fig. 2. Breaker-and-a-half substation scheme.

$$RT = \begin{cases} RT_0 & v_{max} \leq 30m/s \\ RT_0 \times SC_{\sigma 1} & 30m/s < v_{max} \leq 50m/s \\ RT_0 \times SC_{\sigma 2} & 50m/s < v_{max} \leq 60m/s \end{cases} \tag{7}$$

where severity coefficient $SC_{\sigma 1} \sim U(1,2)$, and $SC_{\sigma 2} \sim U(2,4)$ are randomly generated within relevant predetermined ranges.

If all the weather-related outages of lines and towers and their repair times are determined by the wind profiles data and the fragility curves, then the component states of the system can be simulated during the whole sequential MCS period. The detailed steps are depicted in Fig. 4. Furthermore, with some smart grid technologies implemented and some essential power system operation analysis, the system resiliency level enhancement towards the reliability indices and load curtailment information under natural hazard conditions can be evaluated.

3. Demand side management modeling and weather condition based pricing mechanism

This paper presents a weather condition-based pricing mechanism which is incorporated into a real-time pricing program to quantify the contribution of DSM in the enhancement of power system resilience under natural hazard. The DSM model proposed in Ref. [43] is deployed here to model the response characteristics of the customers. The WCRTP mechanism is then established based on the predicted wind speed information of windstorms and the load levels of the system, which is discussed in detail as follows.

3.1. The load economic model of DSM

The definition of price elasticity is the sensitivity of demand with respect to the electricity prices, which is illustrated as follows [63]:

$$E = \frac{r_0}{L_0} \times \frac{\partial L}{\partial r} \tag{8}$$

where E is demand elasticity, L is the load demand, r is the spot electricity price, L_0 is initial load demand and r_0 is the initial electricity price.

The reaction of demand towards the variance of electricity prices can be categorized into two types due to its transferable characteristic. The first kind of load is not transferable from one time to another and can be either on or off. The sensitivity of this kind of load can only be reflected in a single period which is a negative value called "self-elasticity." The load demand function for this kind of load can be expressed as follows.

$$L(m) = \left\{1 + E(m, m) \times \frac{[r(m) - r_0(m) + I(m)]}{r_0(m)}\right\} \times L_0(m) \tag{9}$$

where $L(m)$ is the load demand of time m, $E(m, m)$ is the element in

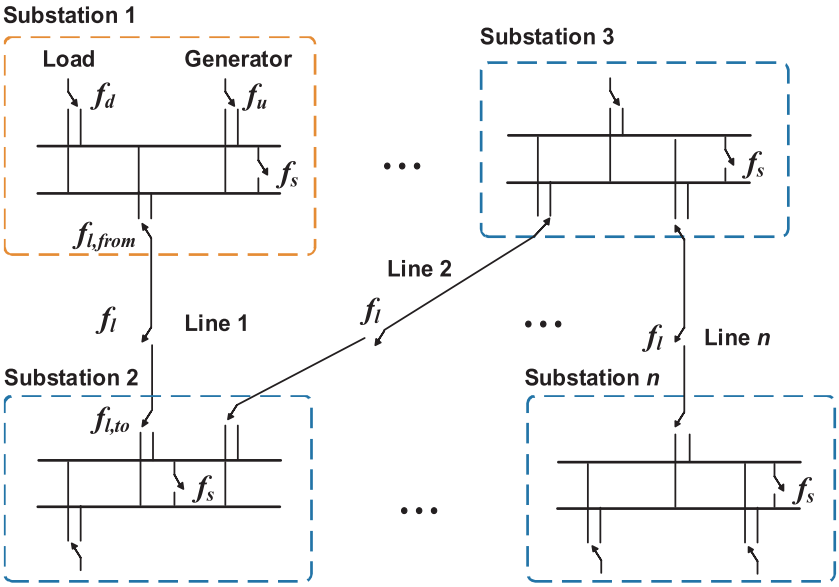

Fig. 3. Generalized model for substations.

the elasticity matrix, and $I(m)$ is the incentive rate ($/MWh) to the load reduction of customer in the m-th hour.

Another kind of load demand can be moved from peak period to flat or valley period, and it has multi-period sensitivity called "cross-elasticity" which is positive. For this kind of load, the load demand function of customer considering both electricity prices and the incentive payment is shown as follows.

$$L(m) = \sum_{\substack{n=1 \\ m\neq n}}^{24} E(m,n)\times\frac{L_0(m)}{r_0(n)} \times [r(n) - r_0(n) + I(n)] + L_0(m) \tag{10}$$

where $E(m, n)$ is the cross-elasticity in the elasticity matrix and $I(n)$ is the incentive payment in the n-th hour.

The comprehensive load economic model with both multi-period and single period elastic loads integration can be represented by the combination of (9) and (10) [43]:

$$L(m)/L_0(m) = 1 + E(m,m) \times \frac{[r(m) - r_0(m) + I(m)]}{r_0(m)} + \sum_{\substack{n=1 \\ m\neq n}}^{24} E(m,n) \times \frac{[r(n) - r_0(n) + I(n)]}{r_0(n)} \tag{11}$$

3.2. Weather condition based real time pricing strategies

Under extreme weather conditions like hurricanes and snowstorms, the transmission lines may trip out and the transmission towers may collapse, which cause great loss to power system. The severe transmission congestion and offline of generating unit will decrease the power supply satisfaction significantly. The damage degree of electricity infrastructure and power interruption cost usually have strong correlation with the severity and sequential characteristic of the natural hazard. Therefore, establishing a weather condition based demand response mechanism which can trace the severity of natural hazard will have a better performance in regulating the electricity usage custom of users and relieve the stress of the power system. The weather condition based real time pricing mechanism is shown as follows:

$$WCP(t) = \alpha_1 + \alpha_2 \times WC^{\frac{L^t_{sys} - L_{avg}}{L_{avg}}} \tag{12}$$

$$WC = \begin{cases} 10 & V_{ave} \le 10m/s \\ 20 + (V_{ave} - 10) & 10m/s < V_{ave} \le 20m/s \\ 30 + (V_{ave} - 20) & 20m/s < V_{ave} \le 30m/s \\ 40 + (V_{ave} - 30) & 30m/s < V_{ave} \le 40m/s \end{cases} \tag{13}$$

where the $WCP(t)$ is the weather condition based real-time price, α_1, α_2 are adjustable price parameters to make the prices commensurate with local electricity prices ranges, WC is the weather condition factor which is relevant to the weather conditions, L^t_{sys} is the system load at time t, L_{avg} is the average load of one day and V_{ave} is the day-ahead predicted average wind speed of windstorm.

Based on this pricing mechanism, more sensitive pricing signal will be applied to regulate the energy consumption behavior of customers according to the day-ahead predicted weather conditions. If the wind speed level is higher, which means the system will suffer from relatively higher component outage level and congestion levels, the pricing in peak hours will be higher and it will become lower in valley period. The customer will reduce their energy consumption during peak hours and transfer some load to valley hours. This will contribute to the peak shaving and valley filling performance. It could be regarded as a self-adaptive measure taken by the operator to strengthen the resilience levels of power system from the customer response side. Furthermore, it can help relieve the system generation inadequacy and coordinate with the load restoration process to recover more vital load which might lead to significant economic and social benefits.

It should be noted that this paper only studies the commonly used RTP program to quantify the contribution of weather condition based DSM mechanism to the enhancement of power system resilience under natural hazard. Some other incentive based DSM program could also be integrated in this framework by adding the weather condition based incentive rate $I(m)$ and punishment rate in (11).

4. Network topology optimization modeling

The network topology reconfiguration technology provides a flexible operation mode for the power system which can relieve the transmission congestions caused by the transmission corridor failure under extreme weathers and help to fast recover part of the load being curtailed. It can be regarded as a potential resilience enhancement strategy in smart grid environment. As mentioned above, line switching and bus splitting are effective mechanisms for the implementation of network topology reconfiguration. In the transmission network, high voltage substations are vital node because they are the medium for the

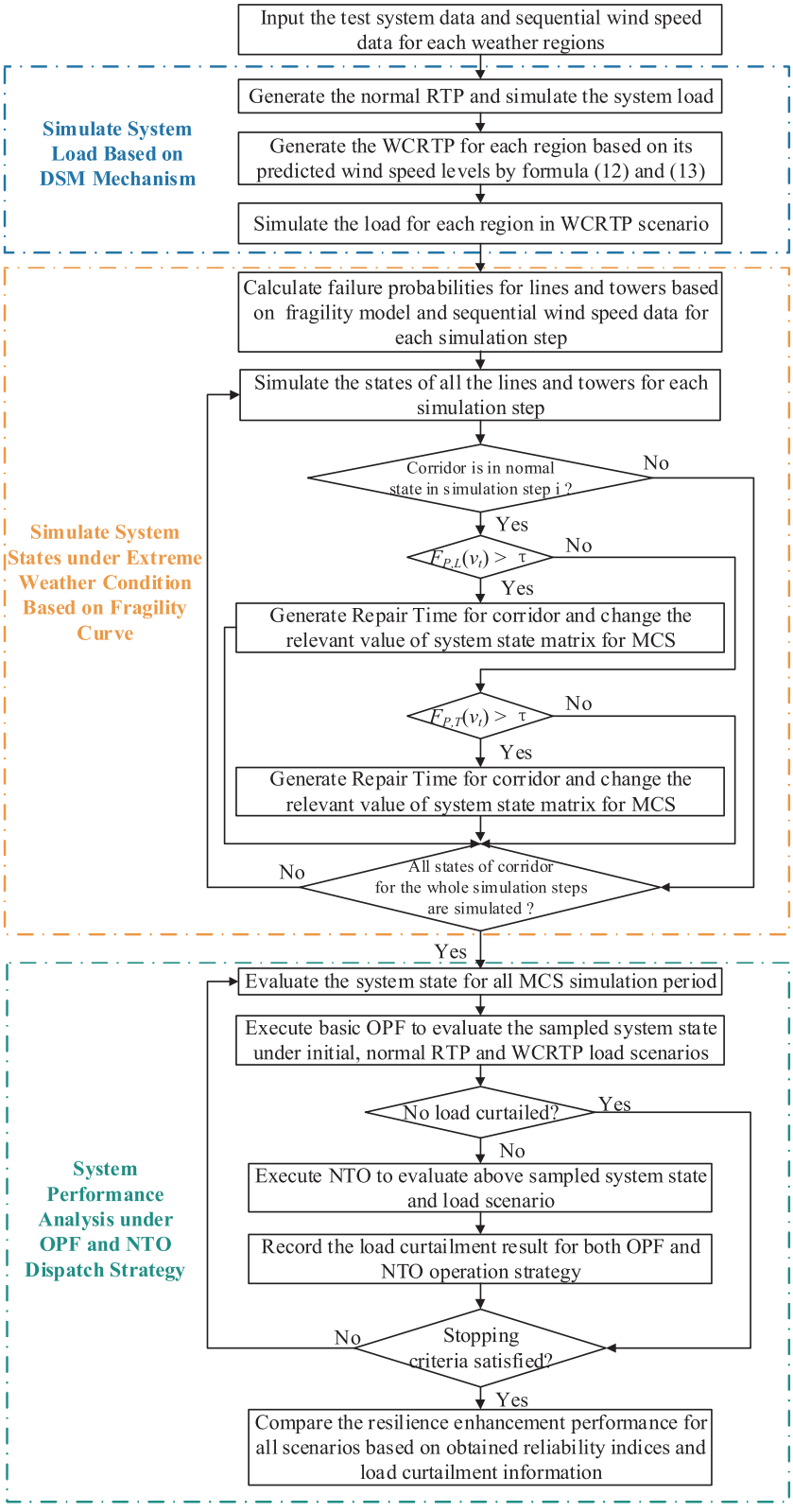

Fig. 4. Flow chart for the analytical procedure.

power delivery from the generating side to multiple levels of customers by transmission lines and for the transformation of voltage classes. Therefore, the structure of substations and the connectivity relationship of elements inside the substations determined by the switching state of circuit breakers within the substation will determine the topology of whole power system. In engineering practice, breaker-and-a-half arrangement is a frequently applied and widely recommended structure for the substation due to its ideal performance in reliability and flexibility, which is shown in Fig. 2.

Based on the analysis of the structure in Fig. 2, a generalized model of substation can be established for the breaker-and-a-half structure, which is depicted in Fig. 3. In substations like substation 1, there are

Table 1
Relevant binary variables with respect to various topology control mechanism.

Busbar splitting mechanism		Line switching mechanism	
Connectivity relationship of two busbars	Relevant binary variable	Switching state	Relevant binary variable
Connected	$f_s = 1$	Switched in	$f_l = 1$
Separated	$f_s = 0$	Switched out	$f_l = 0$

two busbars which could be either connected or separated. The generator, load and transmission lines can connect to either of the busbars. Meanwhile, the transmission line can also be switched in or switched out. The NTO is implemented based on this generalized model. In addition, the relevant binary variables with respect to various topology control mechanism are summarized in Table 1.

Essentially, NTO technology incorporates both transmission line switching and busbar splitting mechanism. It is expressed as a mixed integer linear programming (MILP) problem which is shown as follows [59]. The objective function is formulated in (14), which aims to minimize the load curtailment. It also indicates that the amount of power supply in the power system is maximized.

$$\min\left\{D_{system} - \sum_{d=1}^{N_d}(L_{d,1} + L_{d,2})\right\} \tag{14}$$

where $L_{d,i}$ refers to the load that is connected to busbar i, N_d is the number of loads and D_{system} is the total system load.

The constraints of the optimization problem are shown as follows.

$$0 \le L_{d,1} \le -f_d L_d^{max} + L_d^{max} \quad \forall\, d \tag{15}$$

$$0 \le L_{d,2} \le f_d L_d^{max} \quad \forall\, d \tag{16}$$

$$P_u^{min} - P_u^{min} f_u \le P_{u,1} \le P_u^{max} - P_u^{max} f_u \quad \forall\, u \tag{17}$$

$$P_u^{min} f_u \le P_{u,2} \le P_u^{max} f_u \quad \forall\, u \tag{18}$$

$$P_{l,w,1} + P_{l,w,2} = P_l \quad \forall\, l\, w \in \{from,\ to\} \tag{19}$$

$$|P_{l,w,1}| \le P_l^{max} - f_{l,w} P_l^{max} \quad \forall\, l,\ w \tag{20}$$

$$|P_{l,w,2}| \le f_{l,w} P_l^{max} \quad \forall\, l,\ w \tag{21}$$

$$|P_{l,w,1}| \le f_l P_l^{max} \quad \forall\, l,\ w \tag{22}$$

$$f_{l,w} \le f_l \quad \forall\, l,\ w \tag{23}$$

$$|\varphi_{s,1} - \varphi_{s,2}| \le \varphi^{max} - f_s \varphi^{max} \quad \forall\, s \tag{24}$$

$$\sum_{u \in C_{G,s}} P_{u,1} + \sum_{l \in TL_{to,s}} P_l - \sum_{l \in TL_{from,s}} P_l = \sum_{d \in C_{D,s}} L_{d,1} \quad \forall\, s \tag{25}$$

$$\sum_{u \in C_{G,s}} P_{u,2} + \sum_{l \in TL_{to,s}} P_l - \sum_{l \in TL_{from,s}} P_l = \sum_{d \in C_{D,s}} L_{d,2} \quad \forall\, s \tag{26}$$

$$|(\varphi_{l,from} - \varphi_{l,to})/x_l - P_l| \le V - f_l V \quad \forall\, l \tag{27}$$

$$|\varphi_{l,w} - \varphi_{l,w,1}| \le f_{l,w} \varphi^{max} \quad \forall\, l,\ w \tag{28}$$

$$|\varphi_{l,w} - \varphi_{l,w,2}| \le \varphi^{max} - f_{l,w} \varphi^{max} \quad \forall\, l,\ w \tag{29}$$

$$f_d \le 1 - f_s \quad \forall\, s,\ d \in C_{D,s} \tag{30}$$

$$f_d \le 1 - f_s \quad \forall\, s,\ d \in C_{D,s} \tag{31}$$

$$f_u \le 1 - f_s \quad \forall\, s,\ u \in C_{G,s} \tag{32}$$

$$f_{l,w} \le 1 - f_s \quad \forall\, s,\ w,\ \ l \in TL_{from,s}\ or\ l \in TL_{to,s} \tag{33}$$

$$N_s - \sum_{s=1}^{N_s} f_s \le BST_s^{max} \tag{34}$$

$$N_l - \sum_{l=1}^{N_l} f_l \le LST_l^{max} \tag{35}$$

$$N_l + N_s - \sum_{l=1}^{N_l} f_l - \sum_{s=1}^{N_s} f_s \le TST^{max}$$

In each substation, the relevant load, lines and generators can be connected to either of the busbars. f_d, f_l and f_u are the binary variables of connectivity relationship for load, line and generator respectively. If the value of binary variable is equal to 0, the element is connected to busbar 1 in the corresponding substation; otherwise, if the value is equal to 1, the element is connected to busbar 2.

The connectivity relationship constraints for the load is expressed in (15) and (16). In the constraints, d refers to the index of load demands, $L_{d,i}$ refers to the load that is connected to busbar i, binary variable f_d refers to the relevant busbar that the load demand is connected to and L_d^{max} is maximum amount of load demand d.

Constraints (17) and (18) are associated with the connectivity relationship for the generator and the busbars. In the constraints, u refers to the index of generators, the lower and upper bounds of electric power produced by generator u are symbolized by P_u^{min} and P_u^{max} respectively, $P_{u,i}$ indicates the power that is injected to busbar i from generator u and binary variable f_u refer to the busbar that the generator is connected to.

Constraints (19)–(23) are relevant to the connectivity relationship and switching state for the lines. Constraint (19) illustrates the calculation of power flow summation at each side of transmission line. Constraints (20) and (21) are related to the bus splitting action which lead to different switching states between busbars and each side of lines. Eqs. (22) and (23) refers to the line switching action. In the constraints, l refers to the index for lines, w is the index which describes the ends of lines ($w \in \{from,\ to\}$), f_l describes the state of transmission line switching, binary variable $f_{l,w}$ refers to the busbar that endpoint w of the line is connected to (0: $i = 1$, 1: $i = 2$), P_l refers to the line's power flow, P_l^{max} refers to the maximum value of transmission capacity for line l and $P_{l,w,i}$ is the transmitted power for the endpoint w of line l which is connected to busbar i.

Constraints (24) is associated with the busbars connectivity relationship. In each substation, if two busbars are connected to each other by the circuit breakers, the phase angle difference between two busbars is zero; otherwise, this restriction is not necessary. In the constraints, s refers to the index of substations, φ^{max} refers to the upper bound of allowed voltage angle, f_s is the binary variable which implies whether two busbars are connected or not in corresponding substation s, $\varphi_{s,i}$ refers to the voltage phase angle of the i-th busbar in relevant substation s and i refers to the busbar index ($i \in \{1,\ 2\}$).

In each substation, the power flow balance is associated with (25) and (26). In these equations, $TL_{from,s}$ / $TL_{to,s}$ is the set of transmission lines with their power being transmitted from or to substations s and $C_{D,s}$ and $C_{G,s}$ refer to the sets of load demands and generators in substation s, respectively.

The phase angles differences restrictions are shown in (27)–(29) considering DC power flow theory. In the constrains, $\varphi_{l,w}$ indicates the phase angle at each endpoint of transmission line l, $\varphi_{l,w,i}$ is the phase angle for the i-th busbar of relevant substation which is located at each endpoint of line l and x_l is the reactance of transmission line l and V symbolize a significantly large number.

At each substation, if two busbars are connected to each other, the relevant generators, loads and transmission lines are regarded to be connected to a single busbar. Hence, it is unnecessary to specify the exact busbar the elements are connected to. Some restrictions are applied here to reduce computational complexity, which are shown in (30) and (32).

Some limitations for the number of switching actions are also implemented here. By enforcing constraints (33) and (34), the number of substations which are under separated busbar states and the number of lines which are under switched out states for a given system state can be restricted respectively. The total number of switching actions for both

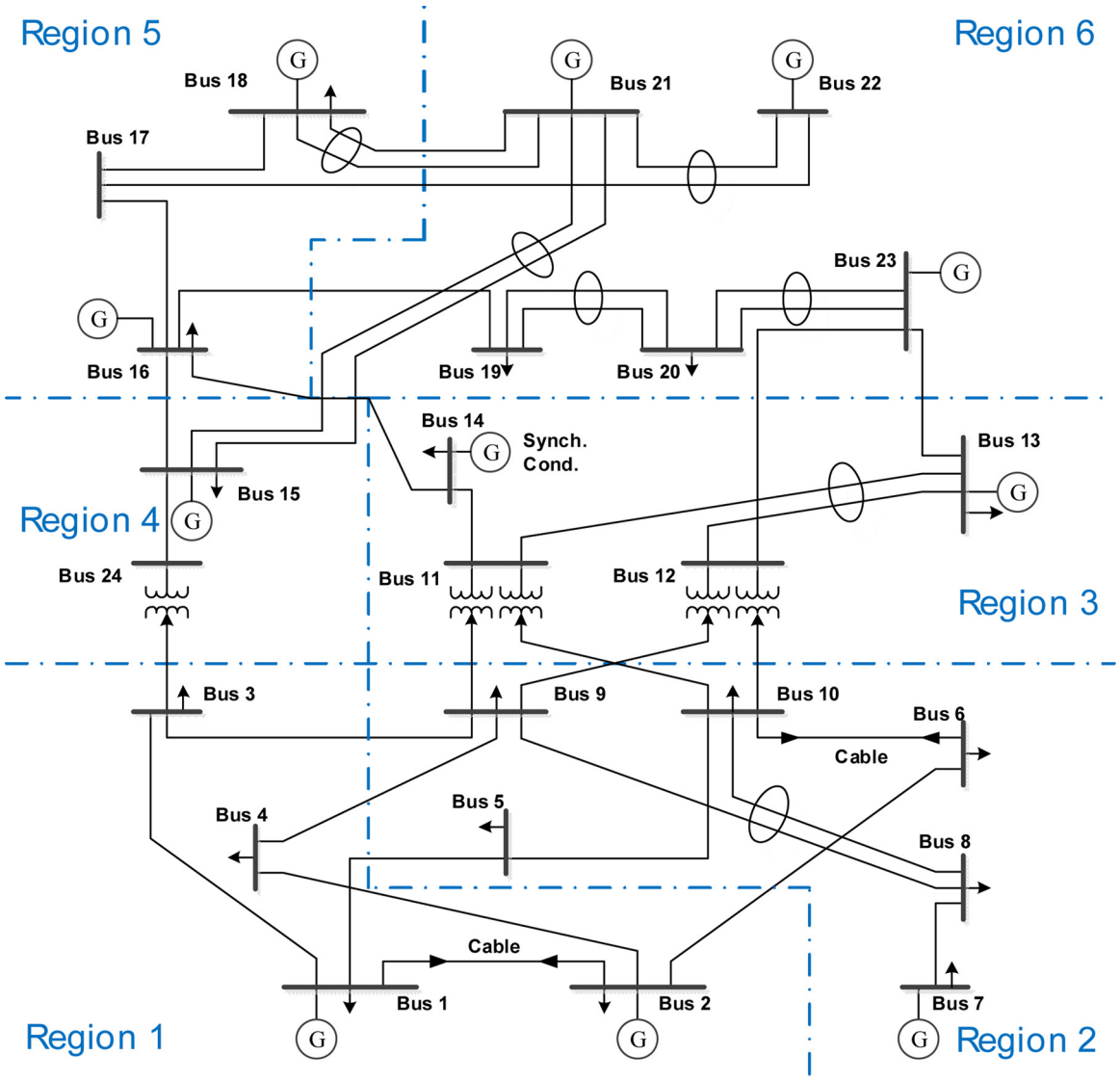

Fig. 5. Weather regions of the IEEE RTS-79 system.

busbar splitting and line switching actions can also be restricted by (35). It is considered all the substations have the bus splitting capability and all the lines have the switching capability. In the constraints, N_s is the total number of substations in the system, N_l is the total number of lines, BST_s^{max} and LST_l^{max} are the upper limit value for available busbar splitting actions and transmission line switching actions for a given system state respectively, TST^{max} is the upper limit value for the total switching action times including both busbar splitting and line switching, f_s and f_l are the binary variables for the switching states of substations and lines respectively, whose values are shown in Table 1.

5. Resilience enhancement evaluation methodology

Based on the DSM model and the NTO model illustrated above, a comprehensive bulk power system resilience enhancement performance evaluation methodology can be established. The DSM and NTO can realize the self-adaptive capability of power system from both customer behavior regulation aspect and transmission system network topology optimization aspect, which can make the system more resilient to the power supply satisfaction when natural hazards happen.

As reliability is one of the key aspects for the definition of a resilient power grid [64] and there are many existing studies using reliability indices to describe the resilience performance of electric power systems [30,31,65], the load curtailment information and the widely used reliability indices such as Loss of Load Probability (LOLP) and Expected Energy Not Supplied (EENS) are deployed in this paper to analyze the resilience enhancement performance of smart grid technologies during a windstorm event, which also enables the comparison between various scenarios when different resilience enhancement measures are deployed. The detailed resilience enhancement evaluation methodology with DSM and NTO incorporated is illustrated as follows.

Firstly, the test system data, fragility curve information and sequential wind speed series are input in the simulation process. The system load levels are simulated under RTP and WCRTP scenarios based on the DSM modeling and corresponding weather condition based pricing mechanism. For the RTP scenario, the weather condition is not considered in this mechanism and its DSM prices are weather independent. So the *WC* factor in (12) is a constant. For the WCRTP scenario, the DSM prices are generated for each region based on its own day-ahead predicted average wind speed of windstorm by (12) and (13). The load information for each region is simulated based on its own DSM prices.

Then the system states under windstorms are simulated. The states of transmission lines and towers are generated by MCS for the whole simulation period according to the fragility curve model, sequential wind speed and generated repair time. The detailed procedure is shown

in Fig. 4. It should be mentioned that new outages of a transmission corridor are not considered during the time when it is being repaired in this study. The state simulation process is accomplished by comparing the sequential failure rate and dynamic random number ($\tau \sim U(0,1)$) based on (5) and (6). Once there is an outage for the transmission line or tower, the repair time will be generated based on (7). All the sequentially sampled system states under extreme weather events will be stored in a system state matrix for further analysis.

Finally, for each sampled system state, resilience enhancement evaluation is performed with both traditional OPF and novel NTO operation strategies incorporated. OPF analysis is applied to calculate the amount of load curtailment for each system state under windstorms. NTO is implemented to realize potential transmission capacity and relieve the transmission congestion by the optimization of network topology. It will help reduce the load curtailment and make the system more resilient against the extreme weather conditions.

To reduce the unnecessary computational burden, for every simulated system state, if the amount of load curtailment calculated by OPF operation strategy is zero, which means all the load demands are satisfied, the NTO will not be executed. Otherwise, NTO will be implemented. The load curtailment information under OPF and NTO circumstance will be recorded in each simulation step.

If sufficient amounts of simulated system states are analyzed to meet the requirement for accuracy, the reliability indices which are applied to quantify the resilient enhancement performance can be calculated based on the recorded amounts of load curtailment for corresponding sampled system states. The flow chart for the analysis procedures is depicted in Fig. 4.

6. Case studies

To evaluate the system resilience enhancement performance of weather condition based demand response program and NTO, the modified IEEE RTS-79 is adopted in the case study [66]. The system is divided into six weather regions and each of them has individual wind profile to reflect the regional characteristic of different weather conditions, which is shown in Fig. 5. The transmission capacity is modified to be 0.6 p.u. A winter week's load profile of the system is applied in the case study. The applied price elasticity matrix is from [43] and the DSM implementation rate is assumed to be 0.1. The failure probability of transmission lines under normal wind speed conditions is considered to be 0.01. $v_{critical\_T}$ and $v_{inevitable\_T}$ are 45 m/s and 150 m/s, respectively [30].

The hourly maximum gusty wind speed profiles of a winter week for six cities around Michigan Lake in the U.S. including Milwaukee, Chicago, Muskegon, Alpena, Toledo and Michigan City are summarized from the database of Great Lakes Environmental Research Laboratory in National Oceanic and Atmospheric Administration (NOAA), which are shown in Fig. 6 [67]. The sequential wind data of six cities are considered as the wind speed profiles in six weather regions.

One purpose of this study is to provide practical and effective guideline for resilience enhancement and management of local utilities in both planning and operational aspects. Therefore, the peak wind gust values of Wisconsin in the U.S. are analyzed for the effective case study design. In Fig. 7, the hurricane force winds gust values of Wisconsin in recent 30 years are summarized (if the value is given by a small estimated interval, the average value is used) [68]. As most of the peak wind gust values are between the range of 30 m/s–55 m/s, six levels of peak wind gusts including 30 m/s, 35 m/s, 40 m/s, 45 m/s, 50 m/s and 55 m/s are tested in the case study to comprehensively study the DSM and NTO performance at multiple maximum wind speed levels. On each level, the sequential wind profiles shown in Fig. 6 are scaled up to the corresponding peak wind gust values. The simulation process will continue until the accuracy requirement of the index is met (i.e., the coefficient of variation for the index of EENS is less than 2.5%).

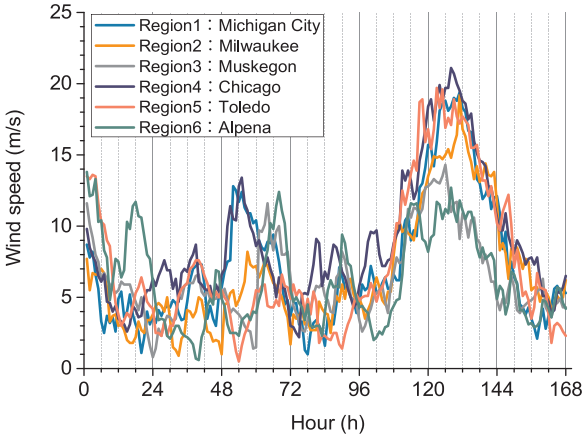

Fig. 6. Wind speed profiles for six cities in a winter week.

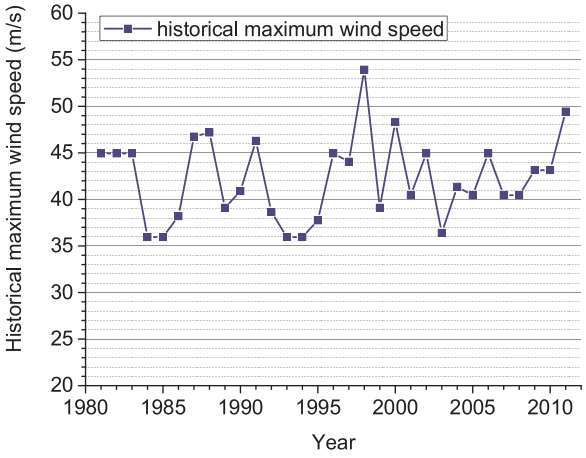

Fig. 7. Peak wind gust values of Wisconsin in the U. S.

6.1. Scenarios analysis

For each peak wind gust level, six scenarios are designed to test the impact of DSM including normal RTP and WCRTP on, and the impact of multiple operation strategies including OPF and NTO on bulk power system resilience enhancement.

1) Initial system load with OPF
2) Initial system load with NTO
3) System load simulated by normal RTP with OPF
4) System load simulated by normal RTP with NTO
5) System load simulated by WCRTP with OPF
6) System load simulated by WCRTP with NTO

The price parameters α_1, α_2 in (12) are set as 0.03$ and 0.1$ respectively to make the real-time pricing within a reasonable range based on the average electricity price in the U.S. (which is considered as 0.1265$ in 2015 according to the report of U.S. Energy Information Administration [69]). The electricity prices under RTP and WCRTP scenarios for each weather region are shown in Fig. 8, and load information simulated under different DSM price scenarios for each region is shown in Fig. 9. The system load profiles under multiple scenarios which are the summation of the regional load profiles are shown in Fig. 10.

It can be verified that the proposed WCRTP mechanism can utilize the predicted wind speed of windstorms to derive effective electricity prices to regulate the energy consumption behavior of customers. As the wind speed in region 4 is relatively higher among all the regions,

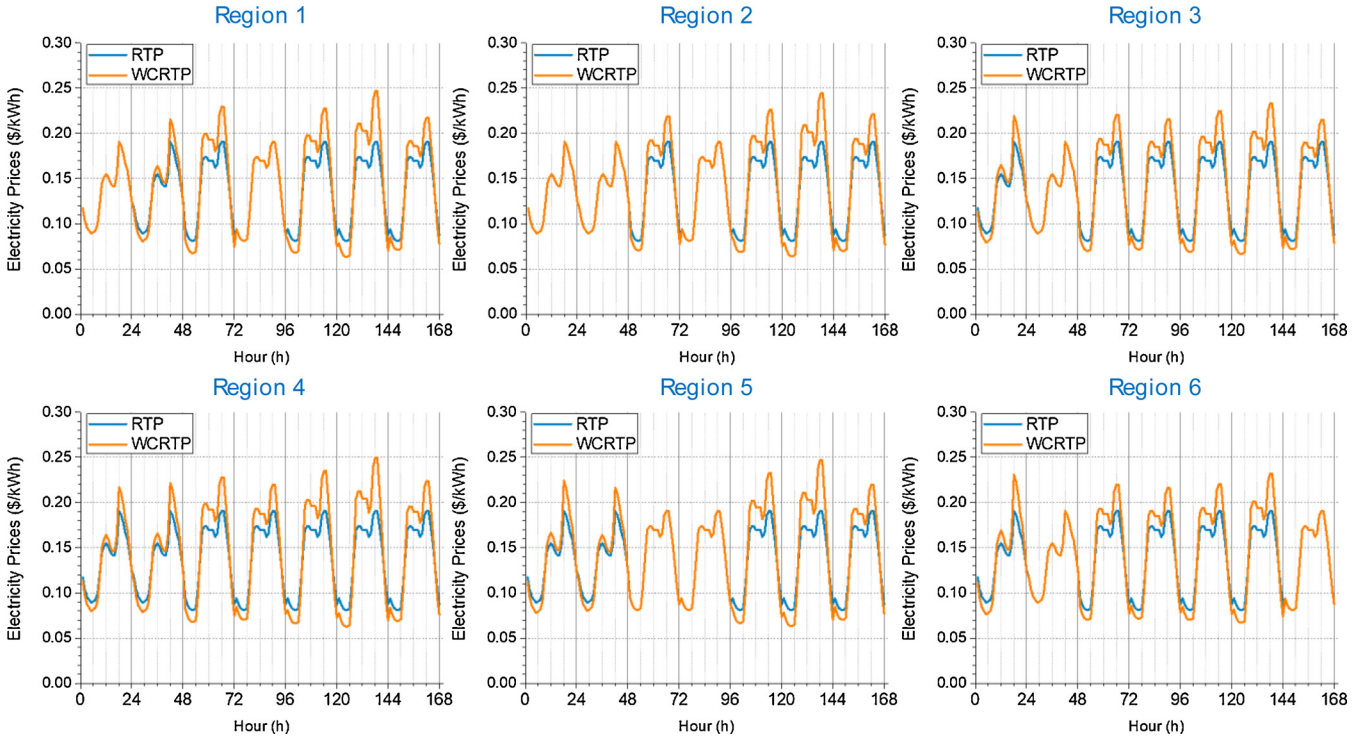

Fig. 8. Electricity prices under RTP and WCRTP scenarios for each region.

the electricity prices under the WCRTP scenario in this region are also very high. The highest price occurs in the fifth day of region 4, which is 0.249 $/kWh. For the day when the average wind speed of windstorm is relatively low, such as the 1st and the 4th day of region 1, the *WC* coefficient in the WCRTP scenario is the same as the normal RTP scenario. So the electricity prices in the normal RTP and WCRTP are the same. From Fig. 8, it can be concluded that the WCRTP can generate more sensitive price signal for each region effectively based on the extreme weather conditions.

In Figs. 9 and 10, the electricity consumption behavior regulation performance for WCRTP is very prominent. The regulation performance is in accordance with the trend of the price signals of DSM. It can be concluded that DSM can help to shave the peak load and transfer part of the load into valley hours effectively, which will help to mitigate the congestions level of power system under extreme weather conditions. In addition, when the severity of windstorm is extremely high during the

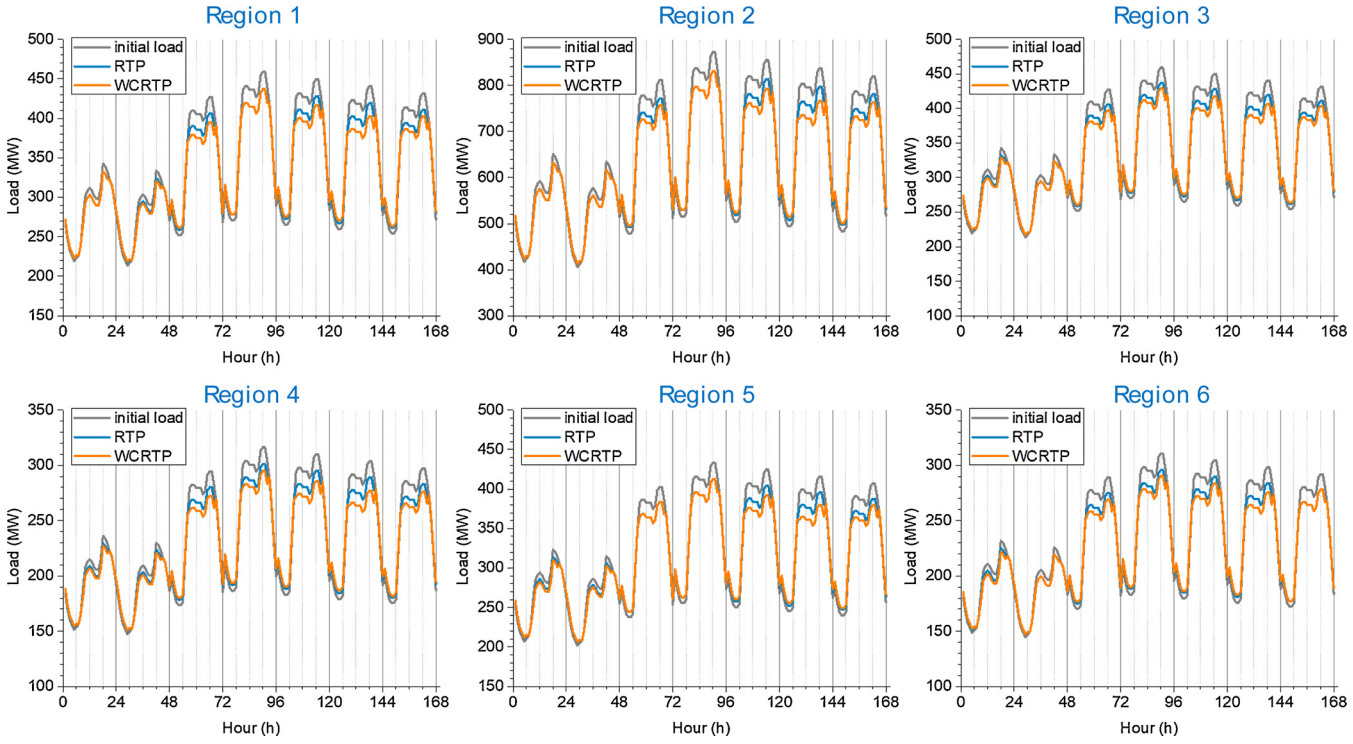

Fig. 9. Load curves under different DSM price scenarios for each region.

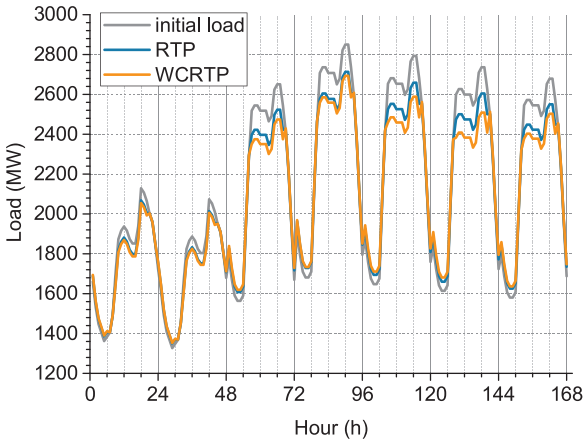

Fig. 10. System load curves under different scenarios.

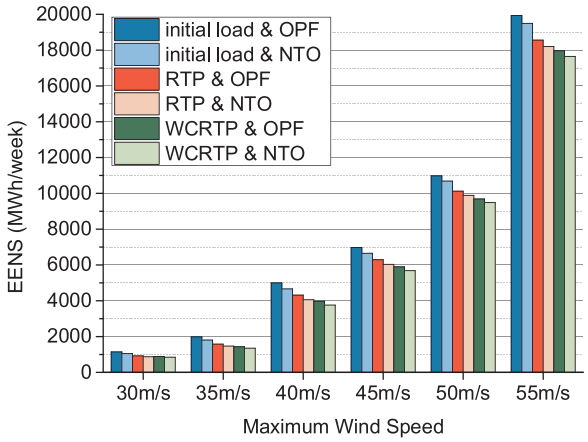

Fig. 12. EENS indices under six scenarios of multiple maximum wind speeds.

5th and 6th day of the week, due to the more sensitive pricing signal which can trace the weather conditions, the WCRTP will have a better energy consumption behavior regulation performance than the normal RTP.

The LOLP and EENS indices under six scenarios of multiple maximum wind speeds levels are depicted in Figs. 11 and 12, respectively. It can be concluded that, in the same operation strategy, most of LOLP indices have a slight decrease under RTP and WCRTP scenarios comparing to the initial state. However, the NTO operation strategy has a prominent performance in the decrease of power outage probability in all initial, RTP and WCRTP load scenarios comparing to OPF. Because it is very hard to change energy consumption behaviors for full recovery from some load curtailment events due to the severe consequences like transmission corridor trips under extreme weather conditions. NTO can help to change the network topology to realize the potential transmission capacity to fully recover some load curtailment, which leads to the decrease of LOLP. As for the EENS, both the DSM programs and the NTO operation strategy show promising performance in the enhancement of EENS. DSM can help to decrease the stress of power systems, increase the generation capacity adequacy and improve the energy supply satisfaction level. This is very meaningful for ensuring the safe operation of power systems under natural hazards because some generating units will be off-line due to the outage of transmission lines, and critical load recovery may require comparatively high generation capacity adequacy. The optimized network configuration from NTO can remove some transmission congestions and decrease the load curtailment which eventually contributes to the improvement of EENS indices and make the system more resilient to the extreme weather conditions.

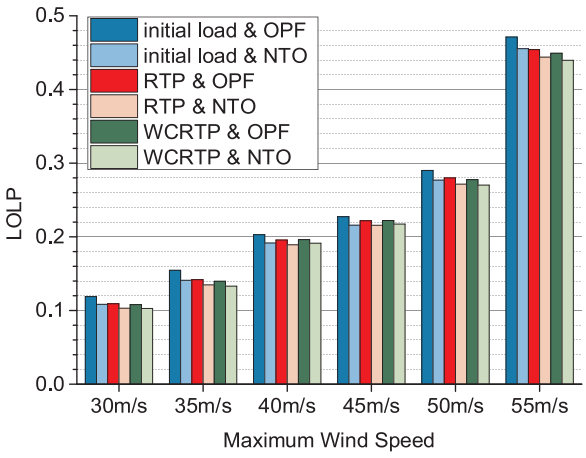

Fig. 11. LOLP indices under six scenarios of multiple maximum wind speeds.

Table 2
EENS improvement rate in different scenarios comparing to OPF & initial load scenario.

Implemented technology	30 m/s	35 m/s	40 m/s	45 m/s	50 m/s	55 m/s
RTP & OPF	19.52%	20.54%	13.62%	9.82%	7.80%	6.88%
WCRTP & OPF	22.24%	27.84%	20.43%	15.48%	11.76%	9.85%
WCRTP & NTO	25.75%	32.01%	24.74%	18.56%	13.59%	11.45%

The EENS improvement rates in different technology implementation scenarios comparing to OPF & initial load scenario are shown in Table 2. It can be seen that the DSM and NTO can contribute to the EENS improvement under all maximum wind speed levels. The WCRTP has a better performance comparing to the conventional RTP due to its weather condition tracing characteristic in its pricing mechanism. When both WCRTP and NTO are implemented, the system performs the best in the electric energy supply aspect which verifies the effectiveness of WCRTP and NTO in the system resilience enhancement.

The performance comparison in Table 3 illustrates the resilience enhancement mechanism of both DSM and NTO technologies under windstorms. It can be concluded that the extreme weather conditions are great threat for the safe operation of the power system because it will cause electric power infrastructure failures and lead to severe consequence like load curtailment. When the DSM program is implemented in the system, the congestion and stress in the power system caused by component failure will be relieved to some extent, so some of load curtailment could be avoided due to the adjustment of load demand pattern by customers. Due to the more ideal customer energy consumption regulation performance based on the weather condition based pricing mechanism, the load curtailment can be further decreased for some given system state. In addition, the implementation of NTO can realize the potential transmission capacity of the transmission infrastructure survived under extreme weathers by optimizing the network topology, so some of the load curtailment are entirely or partly recovered which is a prominent contribution for the system resilience enhancement towards natural hazards like windstorms. The sequential load curtailment profiles under different scenarios are shown Fig. 13. It clearly depicts the sequential load curtailment information of a sampled windstorm event.

The EENS improvement rate under multiple maximum wind speed levels and load scenarios of NTO comparing to OPF is shown in Table 4. The average improvement rate of EENS for 3 load scenarios under 6 maximum wind speed levels are 5.90%, 7.27%, 6.04%, 4.12%, 2.34% and 1.96% respectively. It can be concluded that the NTO can help to improve EENS indices under all maximum wind speed levels and it has a dramatic average EENS improvement rate under 45 m/s, especially on

Table 3
Load curtailment information in different scenarios for some sampled system states.

State	Failed component	Load curtailment (MW)			
		Initial load & OPF	RTP & OPF	WCRTP & OPF	WCRTP & NTO
1	L3, L4, L5, L6, L9, L25, L26, L30, L31, L32, L33, L36	338.71	272.30	224.76	94.69
2	L18, L23, L24, L35	104.51	56.16	31.58	0
3	L11, L18, L20, L22, L24	114.05	74.42	59.33	2.44
4	L5, L11, L12, L18, L24, L27, L33, L38	167.34	119.84	95.70	58.61
5	L3, L4, L8, L9, L11, L13, L23, L24, L25, L26, L27, L29, L32	385.33	322.89	276.17	235.07
6	L3, L5, L6, L8, L11, L12, L24, L25, L28, L29, L33	140.50	101.75	75.70	49.74
7	L3, L4, L9, L11, L12, L21, L23, L25, L27, L28, L29, L31	305.64	255.65	223.17	198.68

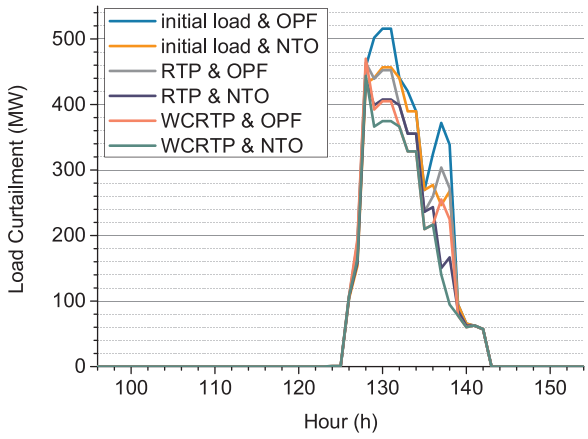

Fig. 13. Sequential load curtailment profiles under different scenarios.

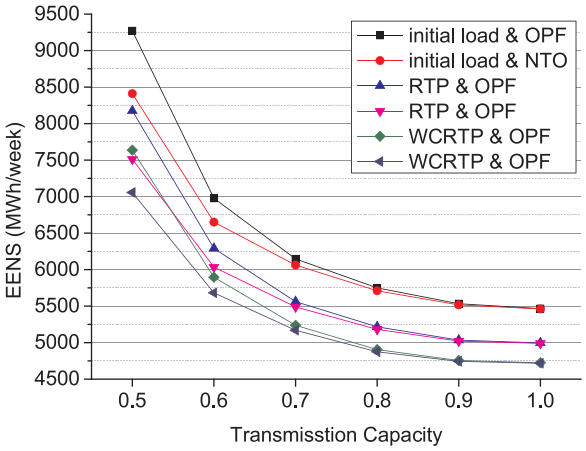

Fig. 14. EENS indices under multiple transmission capacities.

Table 4
Percentage of EENS improvement in NTO integrated scenarios comparing with OPF scenarios.

Load scenario	30 m/s	35 m/s	40 m/s	45 m/s	50 m/s	55 m/s
Initial load	8.26%	9.09%	6.69%	4.67%	2.68%	2.19%
RTP	4.94%	6.97%	6.01%	4.07%	2.28%	1.93%
WCRTP	4.51%	5.77%	5.42%	3.63%	2.07%	1.76%

30 m/s, 35 m/s and 40 m/s. Under high wind speed levels, for example 50 m/s and 55 m/s, the performance is less prominently because more transmission corridors are out of order and there is less potential transmission capacity to be realized. The EENS improvement is relatively high in initial load scenario when the system has more stress comparing to RTP and WCRTP. However, it can be seen that the comprehensive improvement performance of both DSM and NTO perform better in Fig. 13, especially for WCRTP and NTO scenario. The result shown above is the average performance level during the whole simulation period, the result may vary in specific system state.

6.2. Sensitivity analysis

Due to various levels of power grid construction and multiple operating conditions in different regions, the transmission capacity will influence the congestion levels of a power grid under extreme weather conditions and it should be considered in the evaluation process. In addition, the implementation rate of DSM is closely related to the effect of DSM programs on the load levels and its resilience enhancement performance, which should also be considered in the evaluation methodology to quantify its impact. Therefore, the sensitivity analysis of transmission capacity and implementation rate of DSM is illustrated as follows. The wind speed level 45 m/s is applied here to perform the sensitivity analysis.

6.2.1. Transmission capacity

The EENS indices under different transmission capacities for six scenarios are shown in Fig. 14. It can be concluded that the DSM is verified to be an effective resilience enhancement measure for all transmission capacities. The WCRTP has a better performance because its weather tracing characteristic contributes to more effective regulation of customers' energy consumption behavior. As for the NTO, the EENS enhancement performance is better when the system has relative low transmission capacities. The EENS improvement performance is prominent when the transmission capacity is less than 0.8. This helps to prove that NTO is an effective measure for the power systems to be more resilient under extreme weather conditions, especially for those systems which have relatively low transmission adequacy and high congestion levels.

6.2.2. DSM implementation rate

The EENS indices of different DSM implementation rates for six scenarios are depicted in Fig. 15. With the increase of the DSM implementation rate, the reliability indices are also decreased gradually. This is because with more customer signed in the DSM contract, the "peak shaving valley filling" performance are getting better, especially for those system which has high valley-to-peak difference. Some electricity will be saved or be transferred from to peak hours to valley hours. Therefore, the stress of power grid will be decreased and the system adequacy will be improved, which contributes to the resilience enhancement. The more sensitive pricing signal performed by WCRTP can adjust the price mechanism according to the day ahead predicted weather conditions. Therefore, it has a better performance. It should be noted that the RTP is just as a representative for DSM programs to quantify its contribution of making the system more resilient under natural hazard. Other price-based and incentive-based DSM programs can also be implemented in the power system operation. If their pricing and response mechanism are properly determined to trace the extreme weather conditions, they will also have a good performance in the

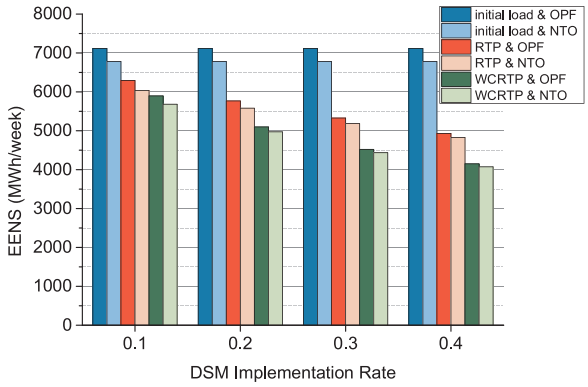

Fig. 15. EENS indices under multiple DSM implementation rates.

resilience enhancement for the power system.

7. Conclusion and future work

This paper conducts a comprehensively study on utilizing DSM and NTO technology to enhance the bulk power system resilience under natural hazard circumstance. The proposed WCRTP mechanism can generate weather condition incorporated DSM prices for each weather region and contribute to the effective regulation for the energy consumption behavior of customers. The NTO can realize the potential transmission capability and reduce the load curtailment under multiple maximum wind speed levels. Sensitivity analysis is performed on multiple transmission capacities and DSM implementation rates of the system. It is proved that NTO is an effective measure to enhance the quality of service of energy supply as well as the resilience level of power systems under extreme weather conditions, especially for the systems which feature relatively low transmission adequacy and high congestion levels. In addition, the resilience enhancement performance from DSM will be enhanced when there is a higher implementation rate.

The proposed weather condition based DSM program and NTO operation strategy are verified to be effective in fully utilizing the self-adaptive capability of power system and potential transmission capacity to mitigate the transmission congestion and make the system more resilient towards extreme weather. The research outcome is a good complement to the existing resilience enhancement measures, which will help the utility to fully use the existing power infrastructure and novel smart grid operation strategy to address the challenge of natural hazards. It can be expected that the proposed measures will be beneficial for the power system resilience enhancement and risk management to relieve adverse impact caused by extreme weather conditions.

For the future work, the extreme weather conditions can be further considered in the pricing mechanism formulation on incentive-based DSM programs and other time-based DSM programs, such as emergency demand response program (EDRP) and critical peak pricing (CPP). The weather condition based competitive DSM contracts and pricing mechanism can help the power system to fully tap the potential of customer response characteristic, which will help enhance the system security and prevent potential cascading failures under extreme events. In addition, the importance of the load can be prioritized and further incorporated in the NTO model. Finally, it is also meaningful to study the coordination of NTO and other emerging transmission system technologies such as dynamic thermal rating in the resilience enhancement applications when a power grid is exposed to extreme weather events.

Acknowledgement

This work was supported by the National Science Fund for Distinguished Young Scholars of China (Project No. 51725701).

References

[1] Office of President Executive Order, Economic benefits of increasing electric grid resilience to weather outages, IEEE USA Books & eBooks, (2013), p. 29.
[2] R.J. Campbell, Weather-related power outages and electric system resiliency, Congr. Res. Serv. Rep. (2012).
[3] A.R. Berkeley III, M. Wallace, C. Coo, A Framework For Establishing Critical Infrastructure Resilience Goals, Final Report and Recommendations by the Council, National Infrastructure Advisory Council, 2010.
[4] M. Chaudry, P. Ekins, K. Ramachandran, et al., Building a Resilient UK Energy System, (2011).
[5] M. Panteli, P. Mancarella, Influence of extreme weather and climate change on the resilience of power systems: impacts and possible mitigation strategies, Electr. Power Syst. Res. 127 (2015) 259–270.
[6] Y. Wang, C. Chen, J. Wang, R. Baldick, Research on resilience of power systems under natural disasters—a review, IEEE Trans. Power Syst. 31 (2) (2016) 1604–1613.
[7] A. Gholami, T. Shekari, M.H. Amirioun, F. Aminifar, M.H. Amini, A. Sargolzaei, Toward a consensus on the definition and taxonomy of power system resilience, IEEE Access 6 (2018) 32035–32053.
[8] H. Nagarajan, E. Yamangil, R. Bent, P.V. Hentenryck, S. Backhaus, Optimal resilient transmission grid design, Power Systems Computation Conference (PSCC) (2016).
[9] W. Yuan, J. Wang, F. Qiu, C. Chen, C. Kang, B. Zeng, Robust optimization-based resilient distribution network planning against natural disasters, IEEE Trans. Smart Grid 7 (6) (2016) 2817–2826.
[10] A. Arab, E. Tekin, A. Khodaei, et al., System hardening and condition-based maintenance for electric power infrastructure under hurricane effects, IEEE Trans. Reliab. 65 (3) (2016) 1457–1470.
[11] S. Ma, B. Chen, Z. Wang, Resilience enhancement strategy for distribution systems under extreme weather events, IEEE Trans. Smart Grid 9 (2) (2018) 1442–1451.
[12] G. Huang, J. Wang, C. Chen, et al., Integration of preventive and emergency responses for power grid resilience enhancement, IEEE Trans. Power Syst. 32 (6) (2017) 4451–4463.
[13] C. Wang, Y. Hou, F. Qiu, et al., Resilience enhancement with sequentially proactive operation strategies, IEEE Trans. Power Syst. 32 (4) (2017) 2847–2857.
[14] M.H. Amirioun, F. Aminifar, H. Lesani, Resilience-oriented proactive management of microgrids against windstorms, IEEE Trans. Power Syst. 33 (4) (2018) 4275–4284.
[15] M.H. Amirioun, F. Aminifar, H. Lesani, Towards proactive scheduling of microgrids against extreme floods, IEEE Trans. Smart Grid 9 (4) (2018) 3900–3902.
[16] Z. Bie, Y. Lin, G. Li, F. Li, Battling the extreme: a study on the power system resilience, Proc. IEEE 105 (7) (2017) 1253–1266.
[17] M. Panteli, D.N. Trakas, P. Mancarella, et al., Boosting the power grid resilience to extreme weather events using defensive islanding, IEEE Trans. Smart Grid 7 (6) (2016) 2913–2922.
[18] S. Lei, J. Wang, C. Chen, Y. Hou, Mobile emergency generator pre-positioning and real-time allocation for resilient response to natural disasters, IEEE Trans. Smart Grid 9 (3) (2016) 2030–2041.
[19] M. Zare, A. Abbaspour, M. Fotuhi-Firuzabad, et al., Increasing the resilience of distribution systems against hurricane by optimal switch placement, Electrical Power Distribution Networks Conference (EPDC) (2017).
[20] S. Yao, P. Wang, T. Zhao, Transportable energy storage for more resilient distribution systems with multiple microgrids, IEEE Trans. Smart Grid (2018).
[21] A. Arab, A. Khodaei, S.K. Khator, et al., Electric power grid restoration considering disaster economics, IEEE Access 4 (2016) 639–649.
[22] H. Gao, Y. Chen, Y. Xu, C. Liu, Resilience-oriented critical load restoration using microgrids in distribution systems, IEEE Trans. Smart Grid 7 (6) (2016) 2837–2848.
[23] C. Chen, J. Wang, D. Ton, Modernizing distribution system restoration to achieve grid resiliency against extreme weather events: an integrated solution, Proc. IEEE 105 (7) (2017) 1267–1288.
[24] A. Gholami, F. Aminifar, A hierarchical response-based approach to the load restoration problem, IEEE Trans. Smart Grid 8 (4) (2017) 1700–1709.
[25] B. Li, R. Roche, A. Miraoui, System resilience improvement using multiple energy supply systems under natural disasters, IECON 2016-42nd Annual Conference of the IEEE Industrial Electronics Society (2016).
[26] S. Clegg, P. Mancarella, Integrated electricity-heat-gas network modelling for the evaluation of system resilience to extreme weather, IEEE PowerTech (2017).
[27] C. Shao, M. Shahidehpour, X. Wang, X. Wang, B. Wang, Integrated planning of electricity and natural gas transportation systems for enhancing the power grid resilience, IEEE Trans. Power Syst. 32 (6) (2017) 4418–4429.
[28] M.H. Amirioun, F. Aminifar, H. Lesani, M. Shahidehpour, Metrics and quantitative framework for assessing microgrid resilience against windstorms, Int. J. Electr. Power Energy Syst. 104 (2019) 716–723.
[29] M. Ouyang, L. Dueñas-Osorio, Multi-dimensional hurricane resilience assessment of electric power systems, Struct. Saf. 48 (2014) 15–24.
[30] M. Panteli, C. Pickering, S. Wilkinson, et al., Power system resilience to extreme weather: fragility modeling, probabilistic impact assessment, and adaptation measures, IEEE Trans. Power Syst. 32 (5) (2017) 3747–3757.
[31] X. Liu, M. Shahidehpour, Z. Li, X. Liu, Y. Cao, Z. Bie, Microgrids for enhancing the power grid resilience in extreme conditions, IEEE Trans. Smart Grid 8 (2) (2017) 589–597.
[32] M. Panteli, P. Mancarella, D. Trakas, et al., Metrics and quantification of operational and infrastructure resilience in power systems, IEEE Trans. Power Syst. 32 (6) (2017) 4732–4742.
[33] M. Panteli, P. Mancarella, Modeling and evaluating the resilience of critical

electrical power infrastructure to extreme weather events, IEEE Syst. J. 11 (3) (2017) 1733–1742.
[34] D.T. Ton, W.T.P. Wang, A more resilient grid: the US Department of Energy joins with stakeholders in an R&D plan, IEEE Power Energy Mag. 13 (3) (2015) 26–34.
[35] Q. Zhang, J. Li, Demand response in electricity markets: a review, 9th IEEE International Conference on the European Energy Market (EEM) (2012).
[36] A. Malik, J. Ravishankar, A review of demand response techniques in smart grids, IEEE Electrical Power and Energy Conference (2016).
[37] Q. Wang, J. Wang, Y. Guan, Stochastic unit commitment with uncertain demand response, IEEE Trans. Power Syst. 28 (1) (2013) 562–563.
[38] P. Babahajiani, Q. Shafiee, H. Bevrani, Intelligent demand response contribution in frequency control of multi-area power systems, IEEE Trans. Smart Grid 9 (2) (2018) 1282–1291.
[39] C.M. Affonso, L.C.P. da Silva, Potential benefits of implementing load management to improve power system security, Int. J. Electr. Power Energy Syst. 32 (6) (2010) 704–710.
[40] R. Sioshansi, W. Short, Evaluating the impacts of real-time pricing on the usage of wind generation, IEEE Trans. Power Syst. 24 (2) (2009) 516–524.
[41] D. Huang, R. Billinton, Impacts of demand side management on bulk system reliability evaluation considering load forecast uncertainty, Electrical Power and Energy Conference (EPEC) (2011).
[42] C.W. Gellings, W.M. Smith, Integrating demand-side management into utility planning, Proc. IEEE 77 (6) (1989) 908–918.
[43] H.A. Aalami, M.P. Moghaddam, G.R. Yousefi, Modeling and prioritizing demand response programs in power markets, Electr. Power Syst. Res. 80 (4) (2010) 426–435.
[44] E. Shayesteh, M.P. Moghaddam, S. Taherynejhad, et al., Congestion management using demand response programs in power market, Power and Energy Society General Meeting-Conversion and Delivery of Electrical Energy in the 21st Century (2008).
[45] D. Huang, R. Billinton, Effects of load sector demand side management applications in generating capacity adequacy assessment, IEEE Trans. Power Syst. 27 (1) (2012) 335–343.
[46] H. Aki, Demand-side resiliency and electricity continuity: experiences and lessons learned in Japan, Proc. IEEE 105 (7) (2017) 1443–1455.
[47] R.P. O'Neill, R. Baldick, U. Helman, et al., Dispatchable transmission in RTO markets, IEEE Trans. Power Syst. 20 (1) (2005) 171–179.
[48] E.B. Fisher, R.P. O'Neill, M.C. Ferris, Optimal transmission switching, IEEE Trans. Power Syst. 23 (3) (2008) 1346–1355.
[49] K.W. Hedman, R.P. O'Neill, E.B. Fisher, et al., Optimal transmission switching with contingency analysis, IEEE Trans. Power Syst. 24 (3) (2009) 1577–1586.
[50] P. Henneaux, D.S. Kirschen, Probabilistic security analysis of optimal transmission switching, IEEE Trans. Power Syst. 31 (1) (2016) 508–517.
[51] E. Nasrolahpour, H. Ghasemi, Congestion management through rotor stress controlled optimal transmission switching, IET Gener. Transm. Distrib. 9 (12) (2015) 1369–1376.
[52] K.W. Hedman, M.C. Ferris, R.P. O'Neill, et al., Co-optimization of generation unit commitment and transmission switching with N-1 reliability, IEEE Trans. Power Syst. 25 (2) (2010) 1052–1063.
[53] J.C. Villumsen, G. Bronmo, A.B. Philpott, Line capacity expansion and transmission switching in power systems with large-scale wind power, IEEE Trans. Power Syst. 28 (2) (2013) 731–739.
[54] A. Khodaei, M. Shahidehpour, S. Kamalinia, Transmission switching in expansion planning, IEEE Trans. Power Syst. 25 (3) (2010) 1722–1733.
[55] M. Lu, H. Nagarajan, E. Yamangil, et al., Optimal transmission line switching under geomagnetic disturbances, IEEE Trans. Power Syst. 33 (3) (2018) 2539–2550.
[56] E. Nasrolahpour, H. Ghasemi, M. Khanabadi, Optimal transmission congestion management by means of substation reconfiguration, Electrical Engineering (ICEE), 20th Iranian Conference on IEEE (2012).
[57] A.A. Mazi, B.F. Wollenberg, M.H. Hesse, Corrective control of power system flows by line and bus-bar switching, IEEE Trans. Power Syst. 1 (3) (1986) 258–264.
[58] W. Shao, V. Vittal, Corrective switching algorithm for relieving overloads and voltage violations, IEEE Trans. Power Syst. 20 (4) (2005) 1877–1885.
[59] M. Heidarifar, H. Ghasemi, A network topology optimization model based on substation and node-breaker modeling, IEEE Trans. Power Syst. 31 (1) (2016) 247–255.
[60] K. Murray, K.R.W. Bell, Wind related faults on the GB transmission network, International Conference on Probabilistic Methods Applied to Power Systems (2014).
[61] R. Billinton, et al., A reliability test system for educational purposes—basic data, IEEE Trans. Power Syst. 4 (3) (1989) 1238–1244.
[62] K.E. Lindsey, Transmission Emergency Restoration Systems for Public Power, Lindsey Manufacturing Co., 2015.
[63] D. Kirschen, G. Strbac, Fundamentals of Power System Economics, Wiley, New York, 2004.
[64] A. Gholami, F. Aminifar, M. Shahidehpour, Front lines against the darkness: enhancing the resilience of the electricity grid through microgrid facilities, IEEE Electrif. Mag. 4 (1) (2016) 18–24.
[65] R. Rocchetta, E. Zio, E. Patelli, A power-flow emulator approach for resilience assessment of repairable power grids subject to weather-induced failures and data deficiency, Appl. Energy 210 (2018) 339–350.
[66] P. Subcommittee, IEEE reliability test system, IEEE Trans. Power Appar. Syst. 6 (1979) 2047–2054.
[67] [Online]. Available: https://www.glerl.noaa.gov/.
[68] [Online]. Available: https://www.crh.noaa.gov/Image/mkx/severe/.
[69] Electric Power Annual 2016, U.S. Dept. Energy, Washington, DC, USA, Tech. Rep., Dec. 2017.
[70] R. Billinton, W. Li, Reliability Assessment of Power Systems Using Monte Carlo Methods, Plenum, New York, NY, U.K, 1994.